

β^- -decay half-lives at finite temperatures for $N = 82$ isotonesF. Minato¹ and K. Hagino²¹*Innovative Nuclear Science Research Group, Japan Atomic Energy Agency, Tokai 319-1195, Japan*²*Department of Physics, Tohoku University, Sendai 980-8578, Japan*

(Received 30 September 2009; revised manuscript received 20 November 2009; published 28 December 2009)

Using the finite-temperature quasiparticle random phase approximation (FTQRPA) on the basis of the finite-temperature Skyrme-Hartree-Fock + Bardeen-Cooper-Schrieffer (BCS) method, we study β^- -decay half-lives for even-even neutron magic nuclei with $N = 82$ in a finite-temperature environment. We find that the β^- -decay half-life first decreases as the temperature increases for all the nuclei we study, although the thermal effect is found to be small at temperatures relevant to r -process nucleosynthesis. Our calculations indicate that the half-life begins to increase at high temperatures for open-shell nuclei. We discuss this behavior in connection to the pairing phase transition.

DOI: [10.1103/PhysRevC.80.065808](https://doi.org/10.1103/PhysRevC.80.065808)

PACS number(s): 23.40.Hc, 21.10.Tg, 26.20.Np, 26.30.Jk

I. INTRODUCTION

β^- decay of neutron-rich nuclei is one of the important subjects for r -process nucleosynthesis. In the r -process, nuclei rapidly capture neutrons and reach the neutron-rich region, until the time scale of neutron capture is comparable to that of the photodisintegration in the vicinity of the neutron shell gaps $N = 50, 82$, and 126. The β^- decay becomes important mainly at this point. It increases the atomic number of neutron-rich nuclei and eventually enables them to continue capturing neutrons again toward heavier nuclei. Therefore, the β^- -decay half-lives of neutron-rich nuclei determine the r -process time scale, and thus considerably influence the final abundance of elements. Likewise, the β^+ decay plays a decisive role in the evolution of the rp -process elements [1].

Most β^- -decay rates of neutron-rich nuclei relevant to the r -process have not yet been measured experimentally. Therefore, r -process calculations have to rely on a theoretical estimate of β -decay half-lives. Several theoretical approaches have been developed so far. One of the most widely used theoretical methods is the gross theory [2], which describes the β -decay rates with a sum-rule approach supplemented by a statistical treatment for final states. Although it has enjoyed considerable success, it is not clear how well the shell and pairing effects for weakly bound systems are treated in the theory. Another approach is the shell model, which successfully reproduces the experimental half-lives of waiting-point nuclei at $N = 50, 82$, and 126 [3–5]. However, a large-scale shell-model calculation for a systematical study for heavy nuclei along the r -process path has been limited so far.

The proton-neutron quasiparticle random phase approximation (pnQRPA) [6–17] is suitable for bridging the gap between the two approaches. Since it is a microscopic approach, the pnQRPA properly takes into account the shell and pairing effects, and moreover, it is ideal for a systematic study. The strength that contributes to the β^- decay mainly comes from a small low-energy tail of the Gamow-Teller (GT) distribution, which is, in general, difficult to reproduce accurately with the pnQRPA. However, the pnQRPA approach based on the microscopic self-consistent mean-field framework has successfully reproduced the β -decay half-lives for neutron-

rich isotopes by appropriately adjusting the proton-neutron pairing strength in the isospin $T = 0$ channel [9–12].

The r -process takes place in an environment of high temperatures ($T \sim 10^9$ K) and high neutron densities ($\rho \geq 10^{20}$ neutrons/cm³). In this environment, a part of the excited states is thermally populated, and in principle, one needs a finite-temperature treatment for β -decay calculations for the r -process. Notice that the thermal effects especially affect low-lying states, which are important for β decay. The thermal effects on the β -decay rates were studied with an independent particle model [18] and with the finite-range droplet model (FRDM) plus gross theory [19]. The temperature dependence of electron capture rates was also studied using large-scale shell-model calculations [5] as well as with the pnRPA with a Skyrme interaction [20].

In this article, we assess the thermal effects on the β decay of neutron-rich nuclei using the pnQRPA approach. A similar attempt was done in Refs. [13,14,21,22], but they used a schematic, separable force for the particle-hole interaction. Some of the authors also neglected the proton-neutron pairing correlation. We instead carry out our calculations based on the finite-temperature Skyrme-Hartree-Fock + Bardeen-Cooper-Schrieffer (BCS) method, together with a contact force for the proton-neutron particle-particle interaction in pnQRPA.

The article is organized as follows. In Sec. II, we summarize the theoretical method for finite-temperature QRPA. In Sec. III, we show the calculated results for the isotones with the neutron magic number $N = 82$, which are relevant to r -process nucleosynthesis. In Sec. IV, we give a summary of the article.

II. THEORETICAL METHODS**A. Finite-temperature Hartree-Fock + BCS method**

To study β decay at finite temperature, we first construct the basis states using the finite-temperature Hartree-Fock + BCS method [23,24]. The formalism of the finite-temperature Hartree-Fock + BCS method is almost the same as that at zero temperature [25–28], except for the particle number and pairing densities. At zero temperature, the single-particle

occupation probability n_i is given by the BCS occupancy v_i^2 . On the other hand, at finite temperatures $\beta = 1/kT$, k being the Boltzmann constant, it is modified to

$$\begin{aligned} n_i(T) &= f_i(T) + \tanh\left(\frac{\beta E_i}{2}\right) v_i^2, \\ f_i(T) &= \langle \alpha_i^\dagger \alpha_i \rangle = \frac{1}{1 + \exp(\beta E_i)}, \end{aligned} \quad (1)$$

where α_i^\dagger and $f_i(T)$ are the creation operator and the occupation probability for a quasiparticle, respectively. $E_i = \sqrt{(\epsilon_i - \lambda)^2 + (\Delta_i)^2}$ is the quasiparticle energy, where ϵ_i and λ are the single-particle energy and Fermi energy, respectively, and the pairing gap Δ_i obeys the gap equation,

$$\Delta_i = -\frac{1}{2} \sum_{j>0} V_{i\bar{i}j\bar{j}} \frac{\Delta_j}{E_j} \tanh\left(\frac{\beta E_j}{2}\right). \quad (2)$$

Here, V is the pairing interaction and \bar{i} is the time-reversed state of i .

Using the densities obtained with the single-particle occupation probabilities n_i , the self-consistent solution is sought by minimizing the free energy,

$$F = E - TS(T), \quad (3)$$

where E is the Hartree-Fock energy and $S(T)$ is the entropy defined as

$$S(T) = -k \sum_i f_i(T) \ln f_i(T) + [1 - f_i(T)] \ln[1 - f_i(T)]. \quad (4)$$

In the following calculations, we use the smooth cutoff scheme for the pairing active space, following Refs. [26,29]. That is, the quasiparticle energy and the gap equation are modified to $E_i = \sqrt{(\epsilon_i - \lambda)^2 + (\gamma_i \Delta_i)^2}$ and

$$\Delta_i = -\frac{1}{2} \sum_{j>0} V_{i\bar{i}j\bar{j}} \frac{\Delta_j}{E_j} \tanh\left(\frac{\beta E_j}{2}\right) \gamma_i, \quad (5)$$

respectively. Here, the cutoff function is defined as [26,29]

$$\gamma_i = \frac{1}{1 + \exp[(\epsilon_i - \lambda - \Delta E)/\mu]}, \quad (6)$$

with $\mu = \Delta E/10$. The variable ΔE is determined to satisfy

$$N_{\text{act}} = \sum_i \gamma_i = N_q + 1.65 N_q^{2/3}, \quad (7)$$

where N_q is the number of particles for protons ($q = p$) or neutrons ($q = n$).

In our calculation, we employ the zero-range density-dependent force,

$$V_{\text{pair}}(\mathbf{r} - \mathbf{r}') = V_q^0 \left(1 - \frac{\rho(\mathbf{r})}{\rho_0}\right) \delta(\mathbf{r} - \mathbf{r}'), \quad (8)$$

for the like-particle (proton-proton and neutron-neutron) pairing interactions. We neglect the proton-neutron pairing for the BCS calculation, although it is taken into account in the QRPA calculation because we are interested in neutron-rich nuclei, rather than $N \simeq Z$ nuclei, in which the proton-neutron pairing plays a minor role. For the parameters for the pairing

interaction in Eq. (8), we fix ρ_0 to be 0.16 fm^{-3} and adjust the strength parameter V_q^0 to reproduce the empirical values for the pairing gap obtained from the three-point mass difference $\Delta^{(3)}(N+1)$ [30].

B. Finite-temperature quasiparticle random phase approximation

Collective motions of hot stable nuclei were studied with the finite-temperature random phase approximation (FTRPA) [31–34]. It was first developed for studying the giant dipole resonance of a hot compound nucleus formed in heavy ion reactions. To discuss the property of hot exotic nuclei, the finite-temperature quasiparticle random phase approximation (FTQRPA) was recently employed in Ref. [35]. The finite-temperature pnQRPA was also developed in Refs. [21,22] for a separable interaction.

The applicability of the FTRPA was assessed with the Lipkin-Meshkov-Glick method [36–39]. These studies showed that the FTRPA works satisfactorily well for the total strength. When the interaction is small so that the ground state is spherical, the FTRPA also yields a reasonable strength function. Since the proton-neutron coupling is usually weak (i.e., the isovector interaction is not large enough to “deform” the ground state in the isospin space), we argue that the finite-temperature pnQRPA provides a reasonable tool to discuss the thermal effects on the β -decay rate.

At finite temperatures, the quasiparticle states are thermally occupied according to the quasiparticle occupancy $f_i(T)$ in Eq. (1). Therefore, the excitations involve both two-quasiparticle excitations and one-quasiparticle one-quasihole excitations, as is schematically shown in Fig. 1. This can be understood as follows (see Fig. 2). At zero temperature, the excited states corresponds to two-quasiparticle states built on the quasiparticle vacuum. At finite temperatures, these excited states are thermally populated. The transitions among the two-quasiparticle states are then described by the operator $\alpha^\dagger \alpha$, for example,

$$\alpha_i^\dagger \alpha_i^\dagger |0\rangle = \alpha_k^\dagger \alpha_j (\alpha_j^\dagger \alpha_i^\dagger |0\rangle). \quad (9)$$

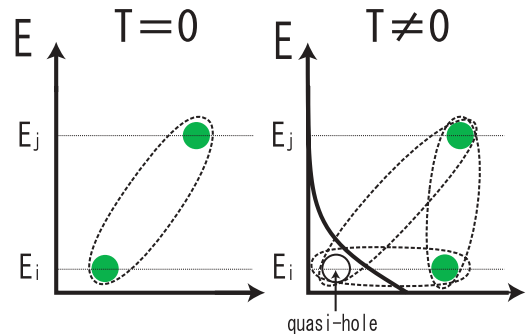


FIG. 1. (Color online) A schematic illustration for the excited states in QRPA. At zero temperature (left panel), excited states correspond to two-quasiparticle (2qp) states, while one-quasiparticle one-quasihole (1qp-1qh) states are also involved at finite temperatures (right panel). The occupation probability of one-quasiparticle states is given by $f_i(T)$ in Eq. (1).

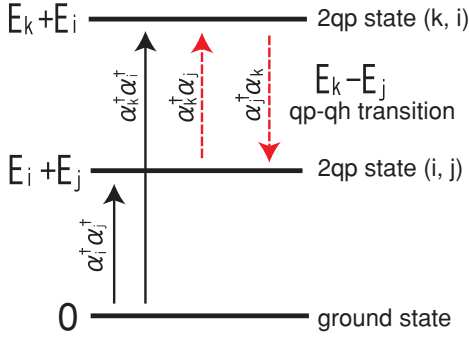


FIG. 2. (Color online) A schematic illustration for the excitation scheme in FTQRPA. Transitions from the ground state correspond to a two-quasiparticle excitation, $\alpha^\dagger \alpha^\dagger$, while the transitions among two-quasiparticle states are described by the operator $\alpha^\dagger \alpha$.

The energy change for this transition is

$$\Delta E = (E_k + E_i) - (E_i + E_j) = E_k - E_j. \quad (10)$$

The transition operator at a finite temperature thus reads [33],

$$Q^\dagger = \sum_{\alpha, \beta} P_{\alpha\beta} \alpha_\alpha^\dagger \alpha_\beta + X_{\alpha\beta} \alpha_\alpha^\dagger \alpha_\beta^\dagger - Q_{\alpha\beta} \alpha_\alpha \alpha_\beta^\dagger - Y_{\alpha\beta} \alpha_\alpha \alpha_\beta, \quad (11)$$

where α and β run over proton and neutron levels, respectively. The first and third terms in Eq. (11) correspond to the transitions among the two-quasiparticle states, which vanish at zero temperature. The QRPA equation can be derived from the equation of motion, $\langle\langle [\delta Q, (H, Q^\dagger)] \rangle\rangle = E_{\text{QRPA}} \langle\langle [\delta Q, Q^\dagger] \rangle\rangle$, where E_{QRPA} is the QRPA excitation energy and δQ is any one-body operator. This yields

$$\begin{pmatrix} \tilde{C} & \tilde{a} & \tilde{D} & \tilde{b} \\ \tilde{a}^T & \tilde{A} & \tilde{b}^T & \tilde{B} \\ -\tilde{D} & -\tilde{b} & -\tilde{C} & -\tilde{a} \\ -\tilde{b}^T & -\tilde{B} & -\tilde{a}^T & -\tilde{A} \end{pmatrix} \begin{pmatrix} \tilde{P} \\ \tilde{X} \\ \tilde{Q} \\ \tilde{Y} \end{pmatrix} = E_{\text{QRPA}} \begin{pmatrix} \tilde{P} \\ \tilde{X} \\ \tilde{Q} \\ \tilde{Y} \end{pmatrix}, \quad (12)$$

where the elements of the matrices \tilde{A} , \tilde{B} , \tilde{C} , \tilde{D} , \tilde{a} , and \tilde{b} are given by Ref. [33],

$$\begin{aligned} \tilde{A}_{\alpha\beta\alpha'\beta'} &= \sqrt{1-f_\alpha-f_\beta} A_{\alpha\beta\alpha'\beta'} \sqrt{1-f_{\alpha'}-f_{\beta'}} \\ &\quad + (E_\alpha + E_\beta) \delta_{\alpha\alpha'} \delta_{\beta\beta'}, \\ \tilde{B}_{\alpha\beta\alpha'\beta'} &= \sqrt{1-f_\alpha-f_\beta} B_{\alpha\beta\alpha'\beta'} \sqrt{1-f_{\alpha'}-f_{\beta'}}, \\ \tilde{C}_{\alpha\beta\alpha'\beta'} &= \sqrt{f_\beta-f_\alpha} C_{\alpha\beta\alpha'\beta'} \sqrt{f_{\beta'}-f_{\alpha'}} \\ &\quad + (E_\alpha - E_\beta) \delta_{\alpha\alpha'} \delta_{\beta\beta'}, \\ \tilde{D}_{\alpha\beta\alpha'\beta'} &= \sqrt{f_\beta-f_\alpha} D_{\alpha\beta\alpha'\beta'} \sqrt{f_{\beta'}-f_{\alpha'}}, \\ \tilde{a}_{\alpha\beta\alpha'\beta'} &= \sqrt{f_\beta-f_\alpha} a_{\alpha\beta\alpha'\beta'} \sqrt{1-f_{\alpha'}-f_{\beta'}}, \\ \tilde{b}_{\alpha\beta\alpha'\beta'} &= \sqrt{f_\beta-f_\alpha} b_{\alpha\beta\alpha'\beta'} \sqrt{1-f_{\alpha'}-f_{\beta'}}, \end{aligned} \quad (13)$$

with

$$\begin{aligned} A'_{\alpha\beta\alpha'\beta'} &= V_{\alpha\beta\alpha'\beta'} (u_\alpha u_\beta u_{\alpha'} u_{\beta'} + v_\alpha v_\beta v_{\alpha'} v_{\beta'}) \\ &\quad + V_{\alpha\beta'\beta\alpha'} (u_\alpha v_\beta u_{\alpha'} v_{\beta'} + v_\alpha u_\beta v_{\alpha'} u_{\beta'}), \\ B_{\alpha\beta\alpha'\beta'} &= V_{\alpha\beta'\alpha'\beta} (u_\alpha v_\beta v_{\alpha'} u_{\beta'} + v_\alpha u_\beta u_{\alpha'} v_{\beta'}) \\ &\quad - V_{\alpha\beta'\beta\alpha'} (u_\alpha u_\beta v_{\alpha'} v_{\beta'} + v_\alpha v_\beta u_{\alpha'} u_{\beta'}), \end{aligned}$$

$$\begin{aligned} C'_{\alpha\beta\alpha'\beta'} &= V_{\alpha\beta'\beta\alpha'} (u_\alpha u_\beta u_{\alpha'} u_{\beta'} + v_\alpha v_\beta v_{\alpha'} v_{\beta'}) \\ &\quad - V_{\alpha\beta\beta'\alpha'} (u_\alpha v_\beta u_{\alpha'} v_{\beta'} + v_\alpha u_\beta v_{\alpha'} u_{\beta'}), \\ D_{\alpha\beta\alpha'\beta'} &= -V_{\alpha\beta\alpha'\beta} (u_\alpha v_\beta v_{\alpha'} u_{\beta'} + v_\alpha u_\beta u_{\alpha'} v_{\beta'}) \\ &\quad + V_{\alpha\beta'\alpha'\beta} (u_\alpha u_\beta v_{\alpha'} v_{\beta'} + v_\alpha v_\beta u_{\alpha'} u_{\beta'}), \\ a_{\alpha\beta\alpha'\beta'} &= V_{\alpha\beta\alpha'\beta} (v_\alpha u_\beta v_{\alpha'} v_{\beta'} - u_\alpha v_\beta u_{\alpha'} u_{\beta'}) \\ &\quad - V_{\alpha\beta'\beta\alpha'} (v_\alpha v_\beta v_{\alpha'} u_{\beta'} - u_\alpha u_\beta u_{\alpha'} v_{\beta'}), \\ b_{\alpha\beta\alpha'\beta'} &= V_{\alpha\beta\alpha'\beta} (v_\alpha u_\beta u_{\alpha'} u_{\beta'} - u_\alpha v_\beta v_{\alpha'} v_{\beta'}) \\ &\quad - V_{\alpha\beta'\beta\alpha'} (v_\alpha v_\beta u_{\alpha'} v_{\beta'} - u_\alpha u_\beta v_{\alpha'} u_{\beta'}). \end{aligned} \quad (14)$$

Using the solution of the QRPA equation, the strength function $S^\pm(E)$ for the GT transition is calculated as

$$\begin{aligned} S^\pm(E_\nu) &= \frac{1}{1 - \exp(-\beta E_\nu)} \left| \sum_{\alpha > \beta} \langle \alpha | \mathcal{O}_{\text{GT}}^\pm | \beta \rangle \right. \\ &\quad \times \left[(u_\alpha u_\beta P_{\alpha\beta}^v + v_\alpha v_\beta Q_{\alpha\beta}^v) \sqrt{f_\beta - f_\alpha} \right. \\ &\quad \left. \left. + (u_\alpha v_\beta X_{\alpha\beta}^v + v_\alpha u_\beta Y_{\alpha\beta}^v) \sqrt{1 - f_\beta - f_\alpha} \right] \right|^2 \\ &\quad \times \delta(E_\alpha - E_\beta - E_\nu), \end{aligned} \quad (15)$$

where $\mathcal{O}_{\text{GT}}^\pm = \sigma \tau^\pm$. For $T = 0$, one can see that Eqs. (12) and (15) are correctly reduced to the usual QRPA equation at zero temperature.

In our calculations, we use the t_0 and t_3 terms in the Skyrme force [40] as the residual interaction,

$$v(\mathbf{r}, \mathbf{r}') = -\chi_s \left(\frac{t_0}{4} + \frac{t_3}{24} \rho^\alpha(\mathbf{r}) \right) (\boldsymbol{\sigma} \cdot \boldsymbol{\sigma}') (\boldsymbol{\tau} \cdot \boldsymbol{\tau}') \delta(\mathbf{r} - \mathbf{r}'), \quad (16)$$

for the GT transition. Our pnQRPA calculation is not fully self-consistent since we do not include all the residual interaction terms in the Skyrme functional. We thus scaled the residual interaction by introducing a scaling factor, χ_s , in Eq. (16). It is determined to reproduce the spurious translational mode (that is, the isoscalar dipole mode) at zero energy at every temperature we consider, with the FTQRPA calculation with a similar residual interaction as in Eq. (16). The resultant χ_s slightly increases as the temperature increases. For instance, at $T = 0.8$ MeV, it increases approximately a few percent from that at $T = 0$ for all the nuclei we calculated. We confirmed that the results do not quantitatively change even if we use a temperature-independent scaling factor.

For the particle-particle matrix elements (with proton-neutron isospin $T = 0$ pairing) in Eq. (14), we use a δ -type interaction,

$$V_{\text{pn}}(\mathbf{r}, \mathbf{r}') = V_{\text{pn}}^0 \delta(\mathbf{r} - \mathbf{r}'). \quad (17)$$

We can regard V_{pn}^0 as a free parameter, as was discussed in Ref. [9], since we do not take into account the $T = 0$ pairing in the Hartree-Fock calculation. The GT low-lying strengths are sensitive to the $T = 0$ pairing, and we adjust the value of V_{pn}^0 to reproduce the known experimental β half-life at zero temperature [9,17].

We solve the QRPA equation by diagonalizing the QRPA matrix in Eq. (12). To include continuum states, we discretize

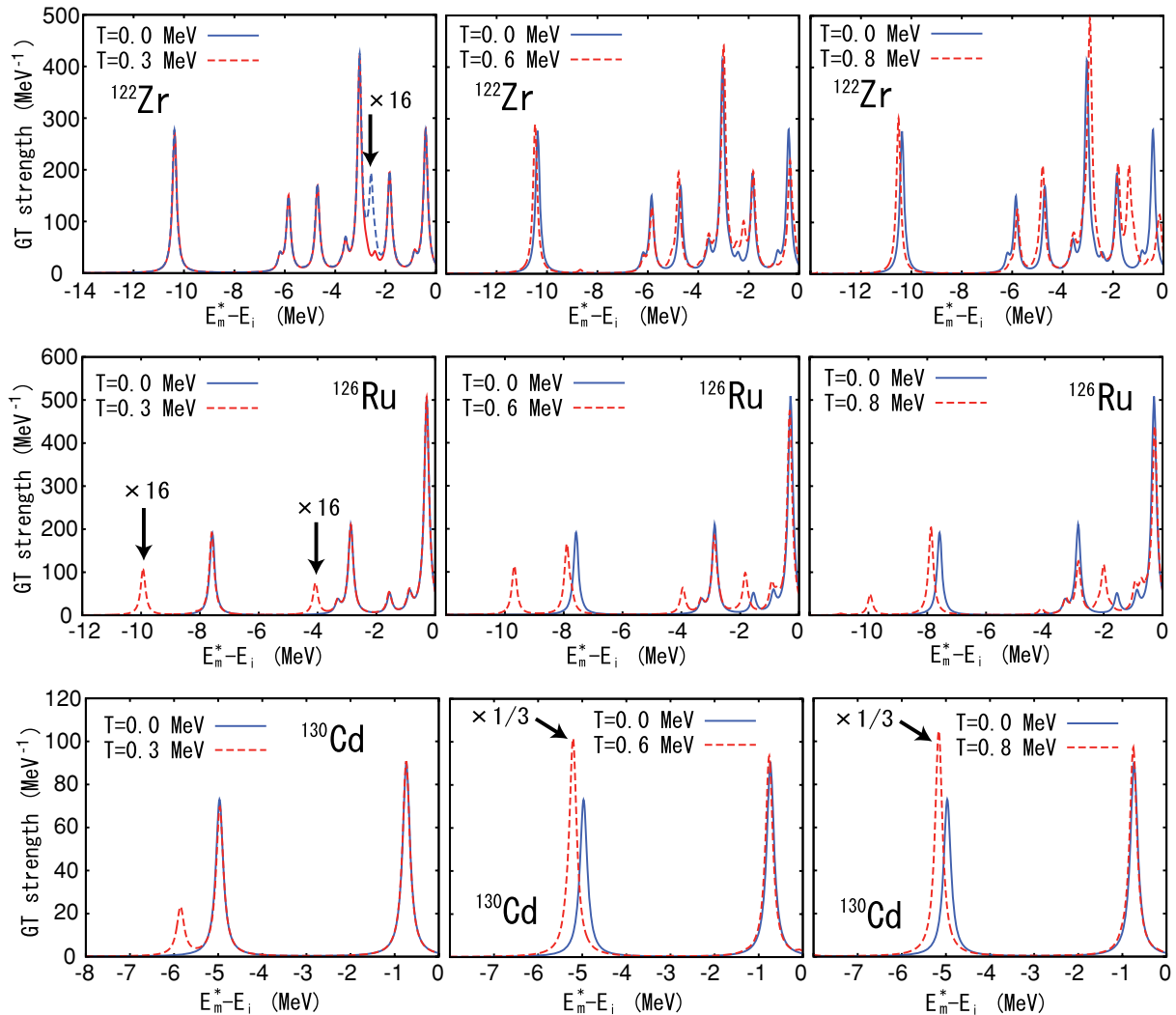


FIG. 3. (Color online) The GT strength functions for the ^{122}Zr , ^{126}Ru , and ^{130}Cd nuclei at $T = 0.3$ (left panels), $T = 0.6$ (middle panels), and $T = 0.8$ MeV (right panels) compared to $T = 0.0$ MeV. These are plotted as a function of $E_m^* - E_i$, where E_i and E_m^* are the energy of the initial and final states, respectively. For ^{126}Ru and ^{122}Zr , the strengths at $T = 0.3$ MeV are scaled by a factor of 16. For ^{130}Cd , the strength at $T = 0.6$ and 0.8 MeV is scaled by one-third.

them with a box boundary condition with a box size of 15 fm. We include the single-particle states up to $\epsilon_{\text{cut}} = 20$ MeV, and we truncate the QRPA model space at the two-quasiparticle energy of $E_{\text{cut}}^{2\text{qp}} = 70$ MeV. We checked the sensitivity of β -decay rates to the model space by using larger ϵ_{cut} and $E_{\text{cut}}^{2\text{qp}}$ and confirmed that the temperature dependence does not change significantly.

III. RESULTS

A. Temperature dependence of GT strengths for $N = 82$ nuclei

Let us now numerically solve the pnQRPA equations and discuss the temperature dependence of the GT strengths for even-even $N = 82$ nuclei, ^{120}Sr , ^{122}Zr , ^{124}Mo , ^{126}Ru , ^{128}Pd , and ^{130}Cd . For this purpose, we mainly use the SLy5 force [41] for the Skyrme parameter set. We set the proton pairing strength $V_p = -1300$ MeV fm $^{-3}$ to reproduce the empirical pairing gap of ^{130}Cd , that is, $\Delta_p^{(3)}(Z + 1) = 0.92$ MeV. The

proton-neutron pairing strength in Eq. (17) is adjusted to $V_{\text{pn}}^0 = -382$ MeV fm $^{-3}$ to reproduce the experimental β -decay half-life of ^{130}Cd (0.162 s) [42], and we use the same value for all the other nuclei.

We find in our results that the strength function is almost the same as that at $T = 0.0$ MeV for temperatures less than $T = 0.2$ MeV, which is considered to be the standard r -process temperature at the initial condition [43]. Figure 3 shows the GT strengths at $T = 0.0$ and at $T = 0.3$ (left panels), $T = 0.6$ (middle panels), and $T = 0.8$ MeV (right panels) for the ^{122}Zr , ^{126}Ru , and ^{130}Cd nuclei as a function of $E_m^* - E_i$, where E_i and E_m^* are the energy of the initial and final states, respectively [see Fig. 4 and Eq. (21)]. Those strength functions are smeared with the Lorentzian function with a width of 0.1 MeV. The strengths at $T = 0.3$ MeV for ^{126}Ru and ^{122}Zr are multiplied by a factor of 16, and at $T = 0.6$ and 0.8 MeV for ^{130}Cd by a factor of 0.3 for presentation purposes. One sees that some new peaks appear at high temperatures, which originate from the

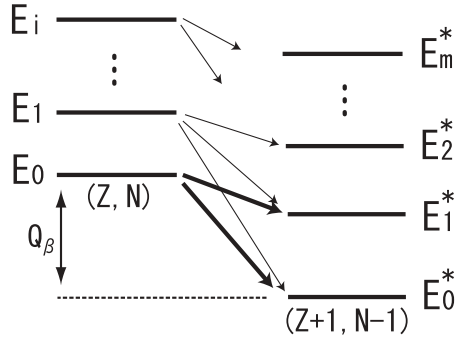


FIG. 4. A schematic illustration for the β^- -decay scheme at finite temperatures. The transitions at zero temperature are indicated by the thick solid arrows; the additional transitions at finite temperatures are indicated by the thin solid arrows.

transition from the excited states. Their strengths for the case of $T = 0.3 \text{ MeV}$ are of the order of 0.1 MeV^{-1} on average, which are approximately 0.1% of the sum rule. Despite its small value, these contributions to the β -decay half-life cannot be neglected as we discuss in the next section.

B. β -decay half-lives

We next calculate the β^- -decay half-lives. Since the contribution of the GT transition to the total β^- -decay rate is much larger than the Fermi transition [44], we take into account only the former. The β -decay half-life $T_{1/2}$ can be calculated with the Fermi golden rule as [9,45]

$$\frac{1}{T_{1/2}} = \frac{\lambda_\beta}{\ln 2} = \frac{G_F^2 g_A^2}{\ln 2 \hbar} \int_0^\infty dE_e \sum_m S^-(E_m) \rho(E_i - E_m^*, E_e), \quad (18)$$

where λ_β is the β -decay rate, $G_F = 1.1658 \times 10^{-11} \text{ MeV}^{-2}$ is the Fermi constant, and $g_A = G_A/G_V$ is the ratio of the vector and pseudo vector constants, which we set as 1.26. The function $\rho(E, E_e)$ is the phase space factor for the outgoing electron and antineutrino and is given by

$$\rho(E, E_e) = \frac{E_e \sqrt{E_e^2 - m_e^2}}{2\pi^3} (E - E_e)^2 F(Z, E_e), \quad (19)$$

where E_e is the energy of the electron and Z is the atomic number of the parent nucleus. $F(Z, E_e)$ is the Coulomb correction factor given by [46]

$$F(Z, E_e) = 2(1 + \gamma)(2k_e R_n)^{2(\gamma-1)} \left| \frac{\Gamma(\gamma + iv)}{\Gamma(2\gamma + 1)} \right|^2 e^{\pi v}, \quad (20)$$

where $\gamma = (1 - Z^2\alpha^2)^{1/2}$ and $v = (Z\alpha E_e/p_e c)$, α being the fine-structure constant. $k_e = p_e/\hbar$ is the electron wave number and $\Gamma(x)$ is the Gamma function. The energy $E_i - E_m^*$ in Eq. (19) is related to the pnQRPA energy E_{QRPA} as [9]

$$E_i - E_m^* \simeq \Delta M_{n-H} - (E_{\text{RPA}} - \lambda_n + \lambda_p), \quad (21)$$

where $\Delta M_{n-H} = 0.78227 \text{ MeV}$ is the mass difference between a neutron and a hydrogen atom.

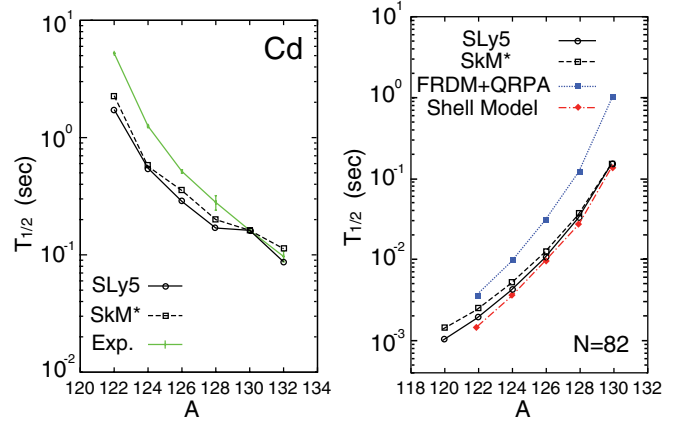


FIG. 5. (Color online) (Left panel): The β -decay half-lives for even-even Cd isotopes at zero temperature. The solid, dashed, and dotted lines show the results with the SLy5, SkM*, and the experimental data [42], respectively. (Right panel): The β -decay half-lives for even-even isotones with neutron number $N = 82$ at zero temperature. The solid and dashed lines show the results of the QRPA with the SLy5 and SkM* parameter sets, respectively. The dotted and dotted-dashed lines show the results of the FRDM + QRPA [7] and the shell-model calculations [3], respectively.

Before we discuss the temperature dependence of β -decay half-lives for even-even isotones with $N = 82$, we check how well our calculation reproduces the experimental known half-lives for $^{122-132}\text{Cd}$ [42] at zero temperature (see Fig. 5). The figure also shows the results with the SkM* parameter set [47] to check the parameter set dependence of the Skyrme functional. The mass number dependence of the half-life is reproduced reasonably well, although our results underestimate the experimental β -decay half-lives by a factor of about 2 to 3 in the low-mass region. We also compare in Fig. 5 our results for the β -decay half-lives for $N = 82$ even-even nuclei at zero temperature with other theoretical approaches, that is, the FRDM + QRPA [7] (the dotted line) and the shell-model calculation [3] (the dashed-dotted line). Notice that there are no experimental data available in this mass region except for ^{130}Cd . We find that our results are in good agreement with the shell-model calculation.

Let us now discuss the temperature dependence of β -decay half-lives. Figure 6 shows the β -decay half-lives normalized to that at zero temperature, $T_{1/2}/T_{1/2}^0$, as a function of temperature T . One sees that, as the temperature increases, the β -decay half-life first decreases gradually for all the nuclei we study for both parameter sets.

One can also see that the temperature dependence is stronger at the larger atomic number. For instance, at $T = 0.8 \text{ MeV}$, the ratio $T_{1/2}/T_{1/2}^0$ is around 0.2 for ^{130}Cd both for the SkM* and SLy5, while it is about 0.9 for ^{120}Sr . This behavior is related to the number of the GT peaks. Figure 3 indicates that the number of GT peaks decreases gradually with atomic number. This is due to the difference between the proton and neutron Fermi surfaces. For ^{130}Cd , the number of GT peaks is only two at $T = 0$, and the thermal effects are relatively large. However, the effects are less significant for ^{122}Zr because there are already many strengths at $T = 0.0 \text{ MeV}$.

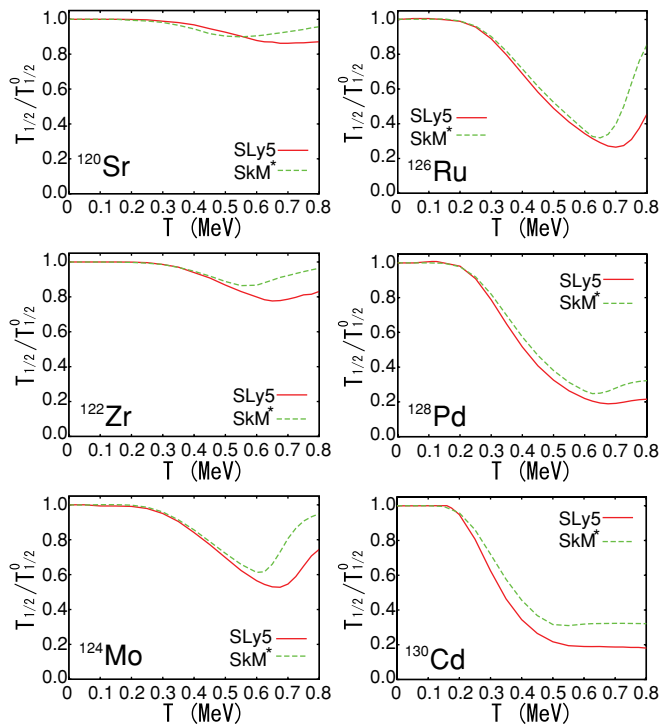


FIG. 6. (Color online) The β -decay half-life $T_{1/2}$ normalized to that at zero temperature, $T_{1/2}^0$. The solid and the dashed lines show the results with the SLy5 and SkM* parameter sets, respectively.

For ^{122}Zr , ^{124}Mo , and ^{126}Ru , the half-lives begin to increase at a temperature around $T = 0.6\text{--}0.7$ MeV. This originates from a subtle interplay between the finite-temperature effects and the pairing effects. In general, the finite-temperature effects decrease the decay half-lives, as indicated in the low-temperature parts in Fig. 3, because of the thermal occupation of the excited states. A similar effect can be expected for the pairing interaction, which scatters particles around the Fermi surface to higher single-particle levels. As the temperature increases, the pairing effect decreases, and eventually the system undergoes the pairing phase transition from the superfluid to the normal fluid phases. This increases the decay half-lives. Depending on which effect is stronger, the temperature dependence of the decay half-lives is determined.

Figure 7 shows the calculated average pairing gaps $\langle \Delta \rangle$. The top and bottom panels show the results of the SLy5 and

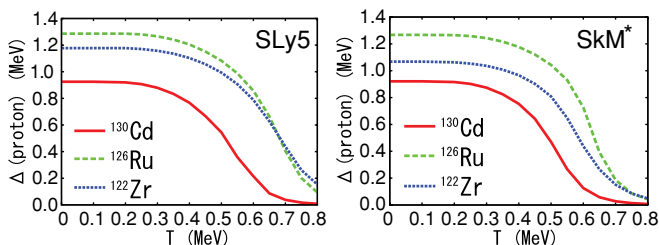


FIG. 7. (Color online) The average proton pairing gap as a function of temperature for the ^{130}Cd , ^{126}Ru , and ^{122}Zr nuclei. The top and bottom panels are results for the SLy5 and SkM* parameter sets, respectively.

SkM* parameter sets, respectively. One sees that the pairing gaps begin to decrease significantly at temperatures of about $T = 0.50\text{--}0.65$ MeV (i.e., the pairing phase transition). For the ^{130}Cd nucleus, being in the neighborhood of the double magic nucleus ^{132}Sn , the pairing gap is smaller than that for ^{126}Ru and ^{122}Zr . Particularly, at $T \sim 0.6$ MeV, the pairing gap is much smaller compared to that for the other two nuclei, and as a consequence, the pairing effect on the decay half-life is much smaller at higher temperatures. This will be a primary reason the decay half-lives have a different temperature dependence between ^{130}Cd and ^{126}Ru or ^{122}Zr nuclei. Note that the critical temperature for the pairing phase transition is lower for SkM* compared to SLy5. This leads to the result that the β -decay half-lives start increasing earlier for SkM* compared to SLy5, as can be seen in Fig. 6.

IV. CONCLUSION

We assess the thermal effects on β -decay half-lives with astrophysical interests for even-even isotones with the neutron magic number $N = 82$. For this purpose, we adopt the FTQRPA method in addition to the finite-temperature Skyrme-Hartree-Fock + BCS method. We use the t_0 and t_3 terms of the Skyrme force for the particle-hole residual interaction and a δ -type interaction for the proton-neutron particle-particle channel in the QRPA formalism.

We calculate the GT strengths in the temperature range from $T = 0.0$ to 0.8 MeV. At finite temperatures, new peaks appear in the strength function due to the transitions from the excited states. From the calculated GT strengths, we evaluate the β -decay half-lives. As the temperature increases, the β -decay half-life decreases gradually for all the nuclei that we studied. We also find that the temperature dependence appears more strongly for nuclei with a larger atomic number. We argue that this is related to the number of GT peaks in the strength function, determined mainly by the difference between the proton and neutron Fermi surfaces. We also find that the β -decay half-life begins to increase at $T > 0.6\text{--}0.7$ MeV for open-shell nuclei as a consequence of the pairing phase transition.

From our results, we conclude that the thermal effect on the β -decay half-life is negligible at the standard r -process temperature, which is considered to be approximately less than 0.2 MeV, at least for even-even $N = 82$ isotones. It will be an interesting future problem to extend the present calculations to odd-mass nuclei, in which the energy of the first excited state is, in general, much smaller than that in even-even nuclei, and thus larger thermal effects may be expected.

ACKNOWLEDGMENTS

We thank G. Colò, T. Kajino, and H. Sagawa for useful discussions. This work was supported by the GCOE program “Weaving Science Web beyond Particle-Matter Hierarchy” at Tohoku University and by the Japanese Ministry of Education, Culture, Sports, Science, and Technology by Grant-in-Aid for Scientific Research under Program No. 19740115.

- [1] R. K. Wallace and S. E. Woosley, *Astrophys. J. Suppl.* **45**, 389 (1981).
- [2] K. Takahashi and M. Yamada, *Prog. Theor. Phys.* **41**, 1470 (1969); T. Tachibana, M. Yamada, and Y. Yoshida, *ibid.* **84**, 641 (1990).
- [3] G. Martínez-Pinedo and K. Langanke, *Phys. Rev. Lett.* **83**, 4502 (1999).
- [4] J. J. Cuenca-García, G. Martínez-Pinedo, K. Langanke, F. Nowacki, and I. N. Borzov, *Eur. Phys. J. A* **34**, 99 (2007).
- [5] K. Langanke and G. Martínez-Pinedo, *Nucl. Phys.* **A673**, 481 (2000).
- [6] J. Krumlinde and P. Möller, *Nucl. Phys.* **A417**, 419 (1989).
- [7] P. Möller and J. Randrup, *Nucl. Phys.* **A514**, 1 (1990).
- [8] I. N. Borzov, S. Goriely, and J. M. Pearson, *Nucl. Phys.* **A621**, 307 (1997).
- [9] J. Engel, M. Bender, J. Dobaczewski, W. Nazarewicz, and R. Surman, *Phys. Rev. C* **60**, 014302 (1999).
- [10] T. Nikšić, T. Marketin, D. Vretenar, N. Paar, and P. Ring, *Phys. Rev. C* **71**, 014308 (2005).
- [11] T. Marketin, D. Vretenar, and P. Ring, *Phys. Rev. C* **75**, 024304 (2007).
- [12] I. N. Borzov, *Phys. Rev. C* **67**, 025802 (2003).
- [13] J.-U. Nabi and H. V. Klapdor-Kleingrothaus, *At. Data Nucl. Data Tables* **88**, 237 (2004).
- [14] J.-U. Nabi and H. V. Klapdor-Kleingrothaus, *At. Data Nucl. Data Tables* **71**, 149 (1999).
- [15] H. Homma, E. Bender, M. Hirsch, K. Muto, H. V. Klapdor-Kleingrothaus, and T. Oda, *Phys. Rev. C* **54**, 2972 (1996).
- [16] A. Staudt, E. Bender, K. Muto, and H. V. Klapdor, *Z. Phys. A* **334**, 47 (1989).
- [17] D. Cha, *Phys. Rev. C* **27**, 2269 (1983).
- [18] G. M. Fuller, W. A. Fowler, and M. J. Newman, *Astrophys. J. Suppl.* **42**, 447 (1980); *Astrophys. J.* **293**, 1 (1985).
- [19] M. A. Famiano, R. N. Boyd, T. Kajino, K. Otsuki, M. Terasawa, and G. J. Mathews, *J. Phys. G: Nucl. Part. Phys.* **35**, 025203 (2008).
- [20] N. Paar, G. Colo, E. Khan, and D. Vretenar, *Phys. Rev. C* **80**, 055801 (2009).
- [21] O. Civitarese, J. G. Hirsch, F. Montani, and M. Reboiro, *Phys. Rev. C* **62**, 054318 (2000).
- [22] O. Civitarese and M. Reboiro, *Phys. Rev. C* **63**, 034323 (2001).
- [23] D. Vautherin, in *Advances in Nuclear Physics* Vol. 22, edited by J. W. Negele and E. W. Vogt (Plenum, New York, 1996).
- [24] A. L. Goodman, *Nucl. Phys.* **A352**, 30 (1981).
- [25] A. L. Goodman, *Nucl. Phys.* **A352**, 30 (1981).
- [26] C. Reiß, M. Bender, and P. G. Reinhard, *Eur. Phys. J. A* **6**, 157 (1999).
- [27] D. Vautherin and D. Brink, *Phys. Rev. C* **5**, 626 (1972).
- [28] D. Vautherin, *Phys. Rev. C* **7**, 296 (1973).
- [29] M. Bender, K. Rutz, P. G. Reinhard, J. A. Maruhn, and W. Greiner, *Phys. Rev. C* **60**, 034304 (1999).
- [30] W. Satula, J. Dobaczewski, and W. Nazarewicz, *Phys. Rev. Lett.* **81**, 3599 (1998).
- [31] D. Vautherin and N. Vinh Mau, *Nucl. Phys.* **A422**, 140 (1984).
- [32] H. Sagawa and G. F. Bertsch, *Phys. Lett.* **B146**, 138 (1984).
- [33] H. M. Sommermann, *Ann. Phys. (NY)* **151**, 163 (1983).
- [34] P. Ring, L. M. Robledo, J. L. Egido, and M. Faber, *Nucl. Phys.* **A419**, 261 (1984).
- [35] E. Khan, N. Van Giai, and M. Grasso, *Nucl. Phys.* **A731**, 311 (2004).
- [36] R. Rossignoli and P. Ring, *Nucl. Phys.* **A633**, 613 (1998).
- [37] T. Hatsuda, *Nucl. Phys.* **A492**, 187 (1989).
- [38] A. I. Vdovin and A. N. Storozhenko, *Eur. Phys. J. A* **5**, 263 (1999).
- [39] K. Hagino and F. Minato, *Phys. Rev. C* **80**, 047301 (2009).
- [40] V. G. Nguyen and H. Sagawa, *Phys. Lett.* **B106**, 379 (1981).
- [41] E. Chabanat, P. Bonche, P. Haensel, J. Meyer, and R. Schaeffer, *Nucl. Phys.* **A635**, 231 (1998).
- [42] G. Audi, O. Bersillon, J. Blachot, and A. H. Wapstra, *Nucl. Phys.* **A729**, 3 (2003).
- [43] S. E. Woosley, J. R. Wilson, G. J. Mathews, R. D. Hoffman, and B. S. Meyer, *Astrophys. J.* **433**, 229 (1994).
- [44] K. Langanke and G. Martínez-Pinedo, *Rev. Mod. Phys.* **75**, 819 (2003).
- [45] M. G. Bowler, *Nuclear Physics* (Pergamon, Headington, Hill Hall, Oxford, 1973).
- [46] H. Behrens and W. Bühring, *Electron Radial Wave Functions and Nuclear Beta-Decay* (Clarendon, Oxford, 1982).
- [47] J. Bartel, P. Quentin, M. Brack, C. Guet, and H. B. Hakansson, *Nucl. Phys.* **A386**, 79 (1982).